Supporting Information

Tailoring Structural Features and Functions of Fullerene Rod Crystals by Ferrocene-Modified Fullerene Derivative

Bohong Jiang,[a#] Qin Tang,[a#] Wenli Zhao,[a] Jiao Sun,[a] Rong An,[a] Tianchao Niu,[a] Harald Fuchs,[a,b] Qingmin Ji[a]*

[a] *Herbert Gleiter Institute of Nanoscience, Nanjing University of Science & Technology, 200 Xiaolingwei, Nanjing 210094, China.*

[b] *Center for Nanotechnology, University of Münster, Wilhelm Klemm-Str. 10, D-48149 Münster, Germany.*

[#] *J.B. and Q.T. contributed equally to this work*

Corresponding Author*: *jiqingmin@njust.edu.cn*

Additional Data

Table S1. The structural features of different fullerene superstructures.

	Lengths(μm)	Diameters(μm)
C_{60}-2IPA	22.5	1
C_{60}-4IPA	10	1
C_{60}-8IPA	7	1
$C_{60}FcC_{60}$-2IPA	5	2
$C_{60}FcC_{60}$-4IPA	3.8	1
$C_{60}FcC_{60}$-8IPA	3.4	1.5

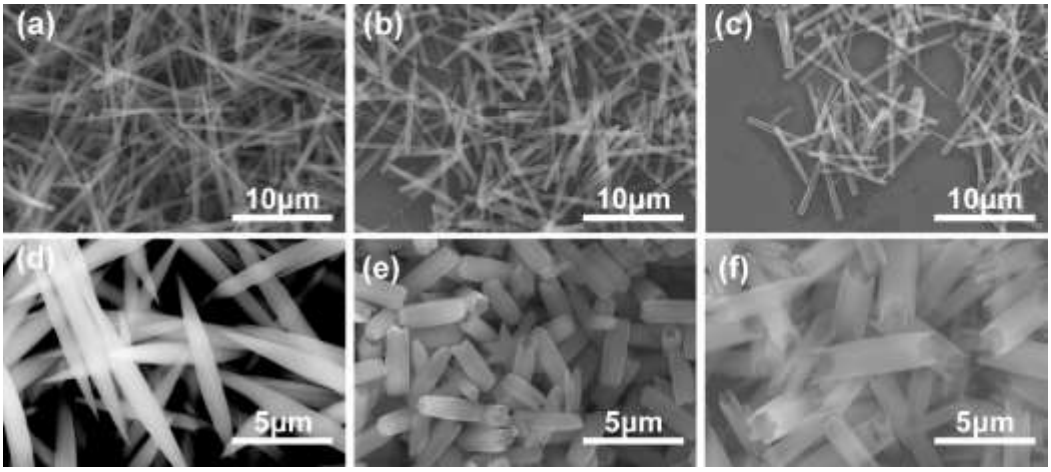

Figure S1. SEM images for C_{60} fullerene superstructures without FcC_{60} of (a) C_{60}-2IPA (nanowhiskers), (b) C_{60}-4IPA (nanowhiskers), (c) C_{60}-8IPA (nanowhiskers); and C_{60} fullerene superstructures with FcC_{60} ($C_{60}FcC_{60}$) of (d) $C_{60}FcC_{60}$-2IPA (spindle-like microrods), (e) $C_{60}FcC_{60}$-4IPA (short tubular microrods), (f) $C_{60}FcC_{60}$-8IPA (microrods with flower-like edge).

Table S2. The structures obtained via LLIP process with different mixing ratios of FcC_{60} and C_{60}.

0 : 1	**0.15 : 9.85**
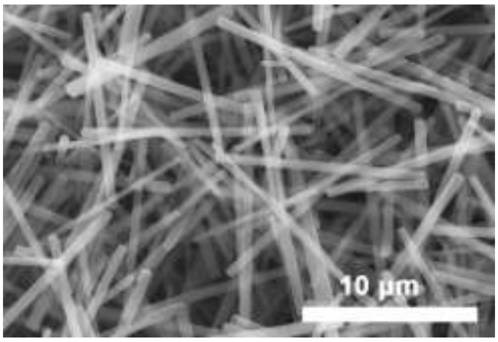	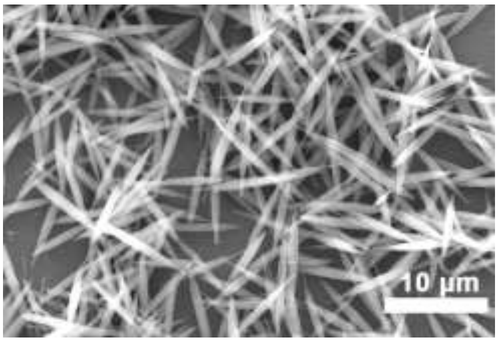
0.3 : 9.7	**0.6 : 9.4**
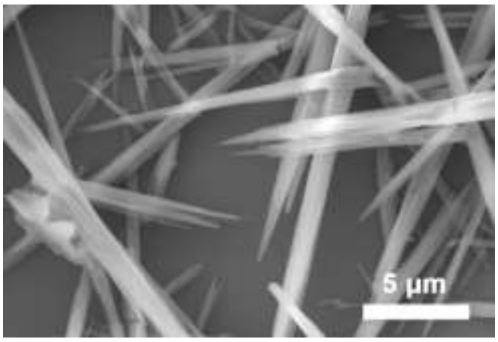	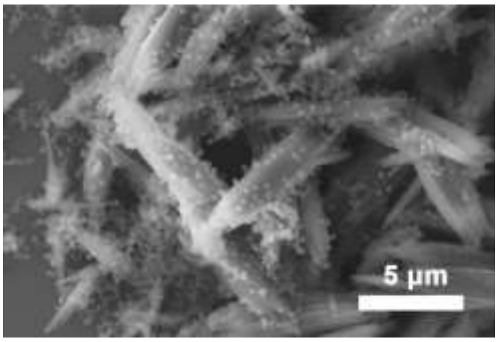
1.2 : 8.8	**2.4 : 7.6**
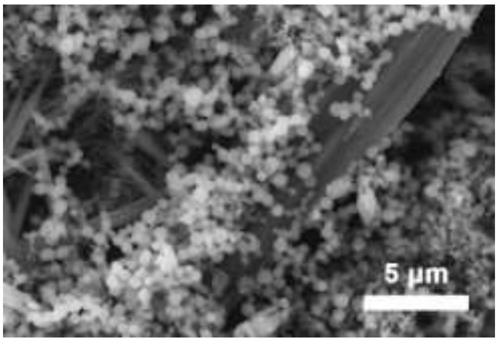	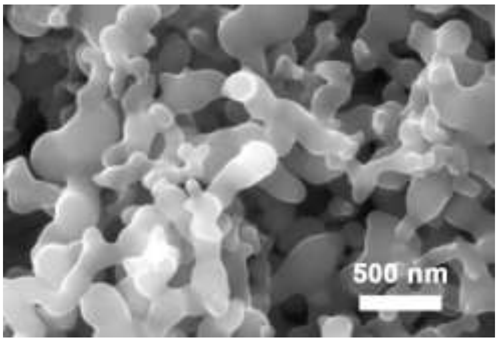

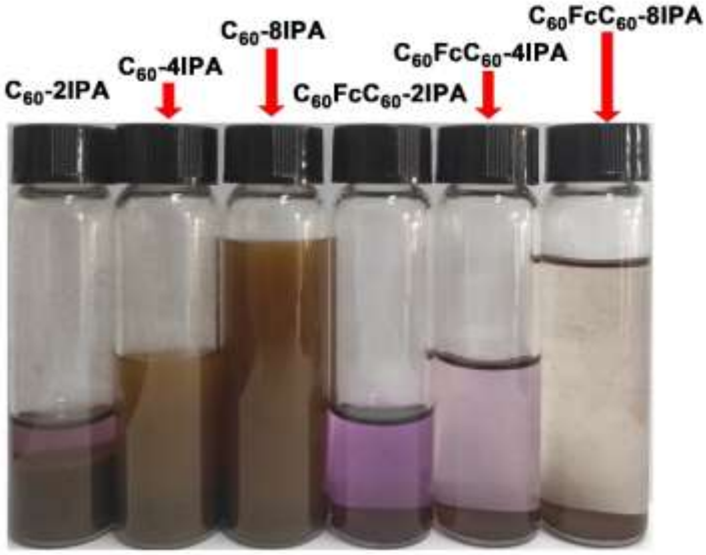

Figure S2. The dispersion appearances of fullerene superstructures by the LLIP process. There are less assembled structures formed and more un-assembled fullerene left in the cases of C_{60}-FcC_{60} mixture system.

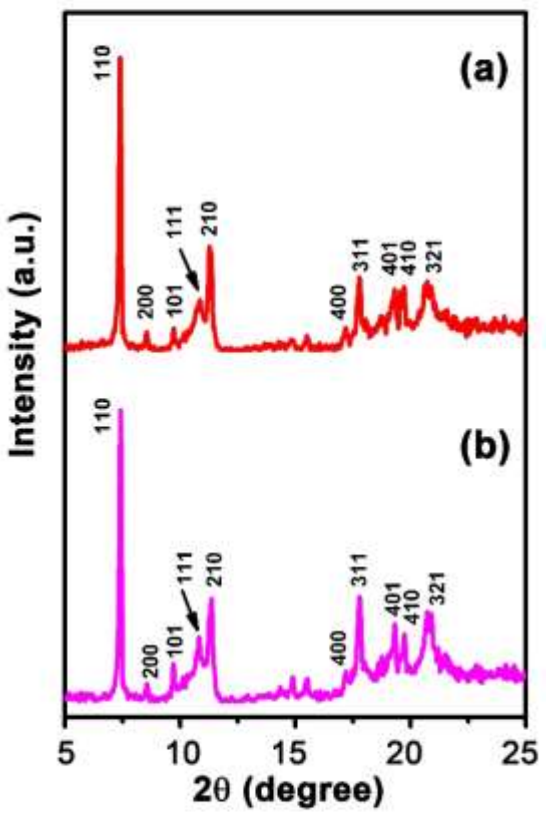

Figure S3. XRD pattern of (a) $C_{60}FcC_{60}$-8IPA, (b) $C_{60}FcC_{60}$-4IPA.

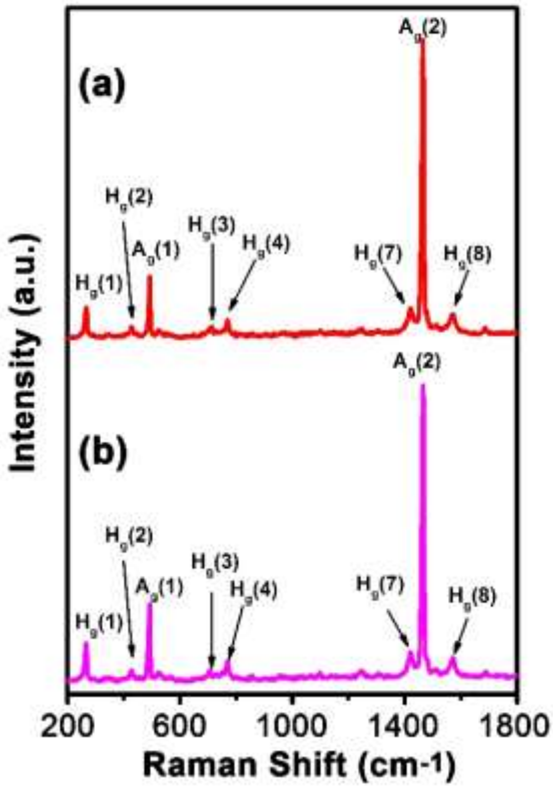

Figure S4. Raman spectra of (a) $C_{60}FcC_{60}$-8IPA and (b) $C_{60}FcC_{60}$-4IPA.

Figure S5. The solubility comparison of C_{60} and FcC_{60}. At the same amount (5 mg) in toluene (2 mL), C_{60}s can not be completely dissolved, while FcC_{60}s are all dissolved.

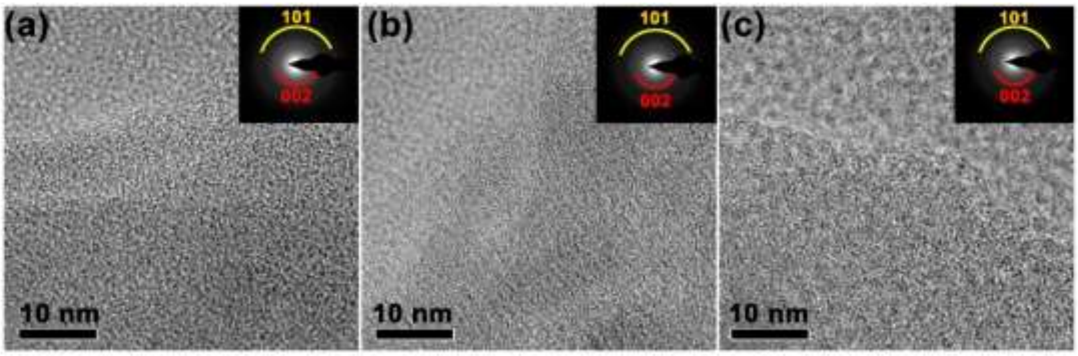

Figure S6. HRTEM images of (g) $C_{60}FcC_{60}$-2IPA_900, (h) $C_{60}FcC_{60}$-4IPA_900, (i) $C_{60}FcC_{60}$-8IPA_900 and inset of panels shows SAED pattern of $C_{60}FcC_{60}$-2IPA_900, $C_{60}FcC_{60}$-4IPA_900 and $C_{60}FcC_{60}$-8IPA_900, respectively.

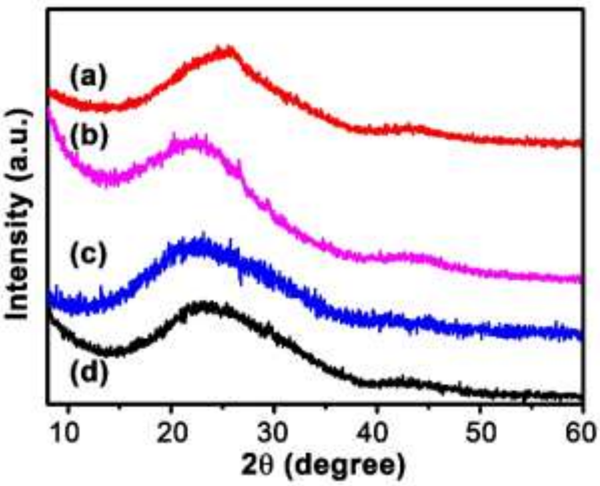

Figure S7. XRD spectra of (a) $C_{60}FcC_{60}$-8IPA, (b) $C_{60}FcC_{60}$-4IPA_900, (c) $C_{60}FcC_{60}$-2IPA_900 and (d) C_{60}-2IPA_900.

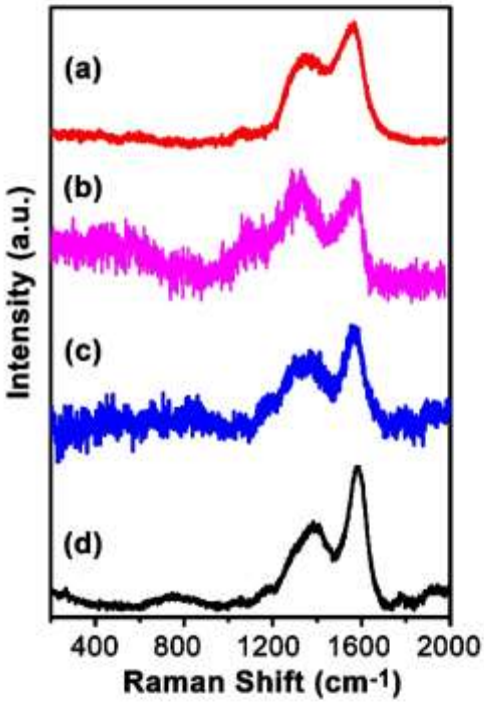

Figure S8. Raman spectra of (a) $C_{60}FcC_{60}$-8IPA, (b) $C_{60}FcC_{60}$-4IPA_900, (c) $C_{60}FcC_{60}$-2IPA_900 and (d) C_{60}-2IPA_900.

Table S3. The porous characters of carbon materials from C_{60} nanowhiskers and various $C_{60}FcC_{60}$ microrods.

	BET surface area (m^2/g)	Average Pore size (nm)	Pore volume (cm^3/g)
C_{60}-2IPA_900	295	2.32	0.059
$C_{60}FcC_{60}$-2IPA_900	491	3.86	0.10
$C_{60}FcC_{60}$-4IPA_900	493	3.86	0.10
$C_{60}FcC_{60}$-8IPA_900	613	3.86	0.11

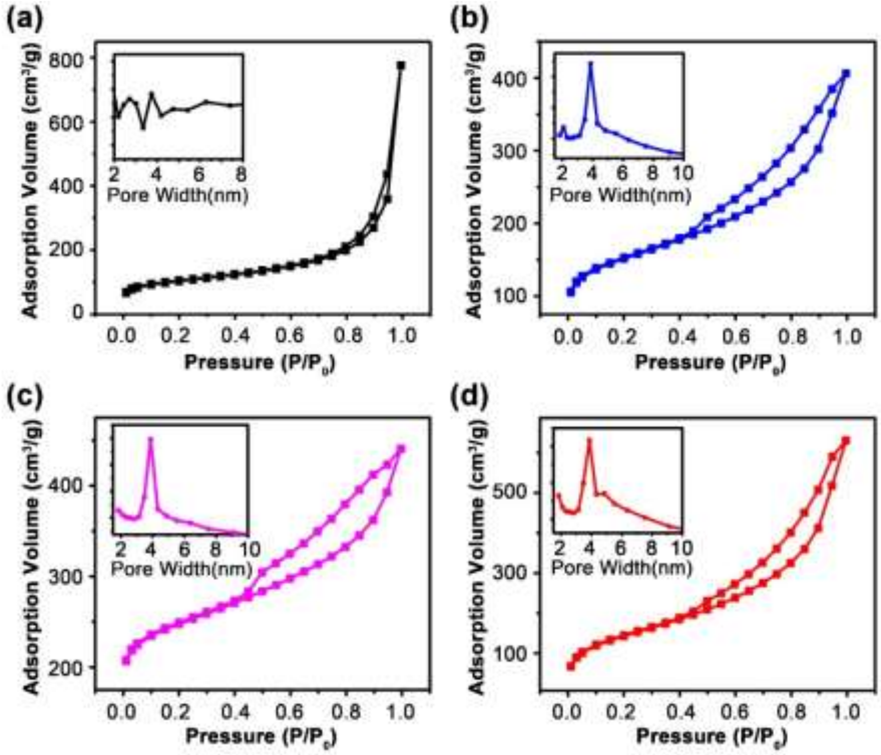

Figure S9. Nitrogen isotherms and pore size distributions (inset) of the porous carbons. (a) C_{60}-2IPA_900, (b) $C_{60}FcC_{60}$-2IPA_900 (c) $C_{60}FcC_{60}$-4IPA_900, (d) $C_{60}FcC_{60}$-8IPA_900.

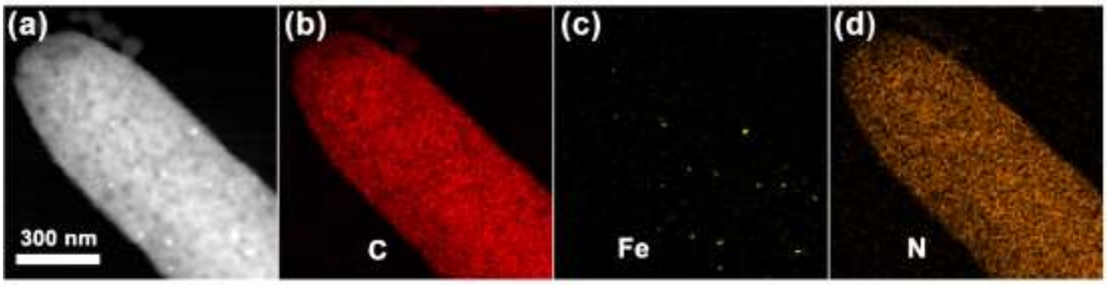

Figure S10. (a) STEM image of the porous carbons from $C_{60}FcC_{60}$ microrods and the elemental mapping of (a) for the (b) C, (c) Fe and N in the microrod.

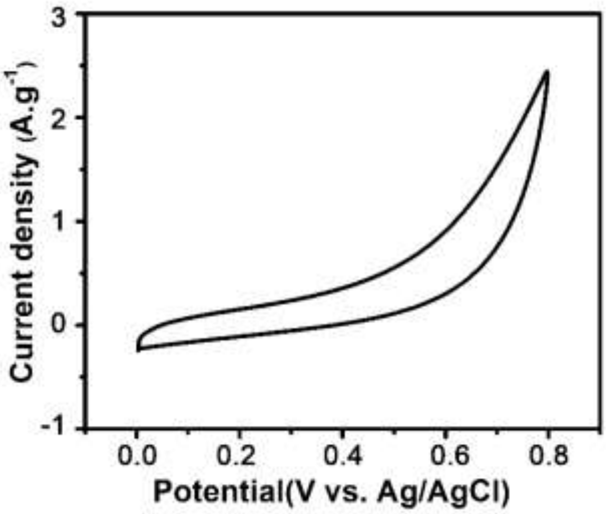

Figure S11. CV curve of the porous carbon from pure C_{60}s (C_{60} nanowhiskers) at a scan rate of 10 mV·s^{-1}.

Table S4. The comparison of the supercapacitor performance with various reported fullerene-derived carbon materials.

Materials	CD (F/g)	CD (A/g)	CV (F/g)	CV (mA/s)	Ref.
C_{60} nanosheet			12.7	5	1
MF C_{60}	141	0.5			2
HT-FNT_2000(C_{60})			145	5	3
HT-FNR_2000(C_{60})			132	5	3
Fe-MFC_{60}-150	112.4	0.1			4
FCL700 (C_{60})	271	1			5
MCFC-900 (C_{70})	205	1	286	5	6
HTFT_2000(C_{70})			212	5	6
HTFT_900(C_{70})			26.4	5	7
C_{60}FcC_{60}-8IPA_900	129	1	102.5	10	this work
C_{60}FcC_{60}-8IPA_900*	261	1	236	10	this work

*Through further activation treatment, we can get better performance C_{60}FcC_{60}-8IPA_900.

Under similar conditions, the same current density or the same cycle speed, C_{60}FcC_{60}-8IPA_900 exhibit a good electrochemical performance at a lower heat treatment temperature.

References (in Table S4)

1. L. K. Shrestha, Y. Yamauchi, J. P. Hill, K. i. Miyazawa and K. Ariga, *J. Am. Chem. Soc.*, 2013, **135**, 586-589.
2. M. Benzigar, S. Joseph, H. Ilbeygi, D. H. Park, S. Sarkar, G. Chandra, S. Umapathy, S. Srinivasan, S. Talapaneni and A. Vinu, *Angew. Chem.Int.Edit.*, 2018, **57**, 569-573.
3. L. K. Shrestha, R. G. Shrestha, Y. Yamauchi, J. P. Hill, T. Nishimura, K. i. Miyazawa, T. Kawai, S. Okada, K. Wakabayashi and K. Ariga, *Angew. Chem.Int.Edit.*, 2015, **54**, 951-955.
4. M. R. Benzigar, S. Joseph, G. Saianand, A. I. Gopalan and A. Vinu, *Micropor. Mesopor. Mat*, 2019, **285**, 21-31.
5. Z. Peng, Y. Hu, J. Wang, S. Liu, C. Li, Q. Jiang, J. Lu, X. Zeng, P. Peng and F. F. Li, *Adv. Energy Mater.,* 2019, **9(11)**, 1802928.
6. P. Bairi, S. Maji, J. P. Hill, J. H. Kim, K. Ariga and L. K. Shrestha, *J. Mater. Chem. A.,* 2019, **7**, 12654-12660.
7. P. Bairi, R. G. Shrestha, J. P. Hill, T. Nishimura, K. Ariga and L. K. Shrestha, *J. Mater. Chem. A.*, 2016, **4**, 13899-13906.